

We are IntechOpen, the world's leading publisher of Open Access books Built by scientists, for scientists

6,900

Open access books available

186,000

International authors and editors

200M

Downloads

Our authors are among the

154

Countries delivered to

TOP 1%

most cited scientists

12.2%

Contributors from top 500 universities



WEB OF SCIENCE™

Selection of our books indexed in the Book Citation Index
in Web of Science™ Core Collection (BKCI)

Interested in publishing with us?
Contact book.department@intechopen.com

Numbers displayed above are based on latest data collected.
For more information visit www.intechopen.com



Redox Flow Batteries: Fundamentals and Applications

Ruiyong Chen, Sangwon Kim and Zhenjun Chang

Additional information is available at the end of the chapter

<http://dx.doi.org/10.5772/intechopen.68752>

Abstract

A redox flow battery is an electrochemical energy storage device that converts chemical energy into electrical energy through reversible oxidation and reduction of working fluids. The concept was initially conceived in 1970s. Clean and sustainable energy supplied from renewable sources in future requires efficient, reliable and cost-effective energy storage systems. Due to the flexibility in system design and competence in scaling cost, redox flow batteries are promising in stationary storage of energy from intermittent sources such as solar and wind. This chapter covers basic principles of electrochemistry in redox flow batteries and provides an overview of status and future challenges. Recent progress in redox couples, membranes and electrode materials will be discussed. New demonstration and commercial development will be addressed.

Keywords: electrochemical energy storage, redox couples, electrolytes, electrodes, membranes

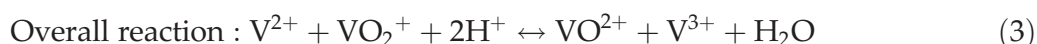
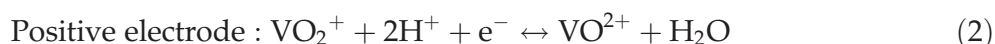
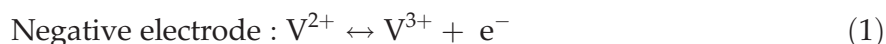
1. Introduction

Global economic growth with the increasing release of carbon dioxide disrupts our ecosystem and causes significant impacts on climate change. An environmentally friendly route to generate electricity from renewable sources such as wind and solar is desirable. To promote the utilization of renewable and sustainable energy and to enhance the stability of grid networks, energy storage systems are needed to store surplus electricity. The stored energy can be then delivered to end customers or to power grids upon need. It is becoming clear that the electrochemical energy storage using rechargeable batteries based on redox chemistry can provide a central solution to tackle such an issue. Through storing energy in recirculating liquid electrolytes, redox flow batteries have merits of decoupled energy density (tank size, electrolyte concentration, cell voltage and number dependent) and power generation capability (electrode size and reaction kinetics dependent). In terms of cost, system flexibility, quick response and

safety concerns for large-scale applications, redox flow batteries show great advantages over other types of batteries such as lead-acid and lithium-ion batteries and are expected to have increasing commercial space through technological development in future. Therefore, the redox chemistry and technical fundamentals of flow batteries, which determine the technological success and market penetration, need to be well understood.

2. Classic vanadium redox flow batteries

Among various flow batteries, vanadium redox flow battery is the most developed one [1]. Large commercial-scale vanadium redox flow batteries are currently in construction. The structure and charge-discharge reactions of vanadium redox flow batteries are schematically shown in **Figure 1**. During discharging, reduction occurs at the cathode and oxidation occurs at the anode as shown in Eqs. (1)–(3) (discharge: \rightarrow , charge: \leftarrow). While these redox reactions occur, proton ions diffuse across the membrane and electrons transfer through an external circuit.



The standard cell voltage for the all-vanadium redox flow batteries is 1.26 V. At a given temperature, pH value and given concentrations of vanadium species, the cell voltage can be calculated based on the Nernst equation:

$$E = 1.26 \text{ V} - \frac{RT}{F} \ln \left(\frac{[VO_2^{+}] \cdot [V^{3+}]}{[VO^{2+}] \cdot [H^{+}]^2 \cdot [V^{2+}]} \right) \quad (4)$$

where R , T and F are the universal gas constant, absolute temperature and Faraday constant, respectively. The crossover of vanadium ions through the membrane may occur, resulting in self-discharge with the unwanted mixing of vanadium species at both sides of the cell, as following [2]:

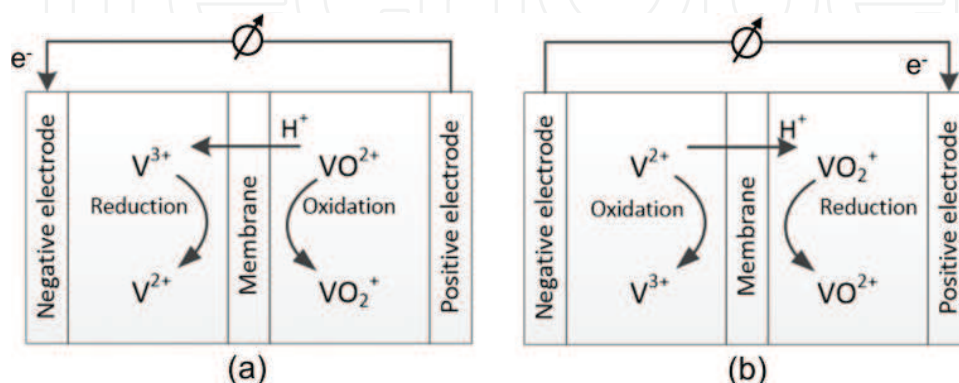
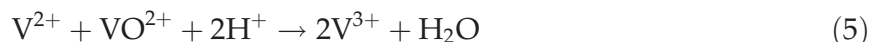
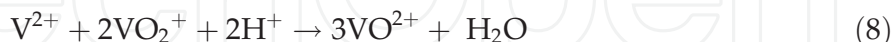


Figure 1. A schematic of a vanadium redox flow battery: (a) charge reaction and (b) discharge reaction.

At the negative electrode:



At the positive electrode:



Side reactions such as hydrogen evolution due to water decomposition and CO_2 evolution due to the oxidation of carbon-based electrode may occur during operation [3]. The battery performance is generally evaluated with three efficiencies: coulombic efficiency (CE), voltage efficiency (VE) and energy efficiency (EE), which are defined as following:

$$\text{CE} = \frac{\text{discharge capacity}}{\text{charge capacity}} \times 100\% \quad (11)$$

$$\text{VE} = \frac{\text{average discharge voltage}}{\text{average charge voltage}} \times 100\% \quad (12)$$

$$\text{EE} = \text{CE} \times \text{VE} \quad (13)$$

The CE reduces because of crossover of vanadium ions during cell operation and side reactions. The VE is related to the operation current density, ionic conductivity of membrane, electrode materials, flow rate and mass transport of electrolyte. As current density increases, the VE reduces due to the increase in polarization.

3. Types and configurations of redox flow batteries

Conventional redox flow batteries have two divided electrolyte reservoirs (**Figure 2a**). Catholyte and anolyte are separated by a membrane, which permits ions to pass through it. The most common working ions in aqueous media, H^+ ($349.8 \text{ S cm}^2 \text{ mol}^{-1}$) and OH^- ($198.0 \text{ S cm}^2 \text{ mol}^{-1}$), have the highest limiting molar conductivity among all known cations and anions, respectively [4]. All-vanadium redox flow batteries, for instance, have $\text{V}^{3+}/\text{V}^{2+}$ redox reactions on the negative side (anolyte) and $\text{VO}_2^+/\text{VO}^{2+}$ on the positive side (catholyte). Such battery uses the same metal ions on both sides. Crossover of metal ions through the membrane will then not cause contamination of the electrolyte. In contrast, for redox flow batteries with different metal ions such as $\text{Fe}^{3+}/\text{Fe}^{2+}$ and $\text{Cr}^{3+}/\text{Cr}^{2+}$ in an iron-chromium flow battery, the cross-contamination via ion penetration may cause irreversible performance loss.

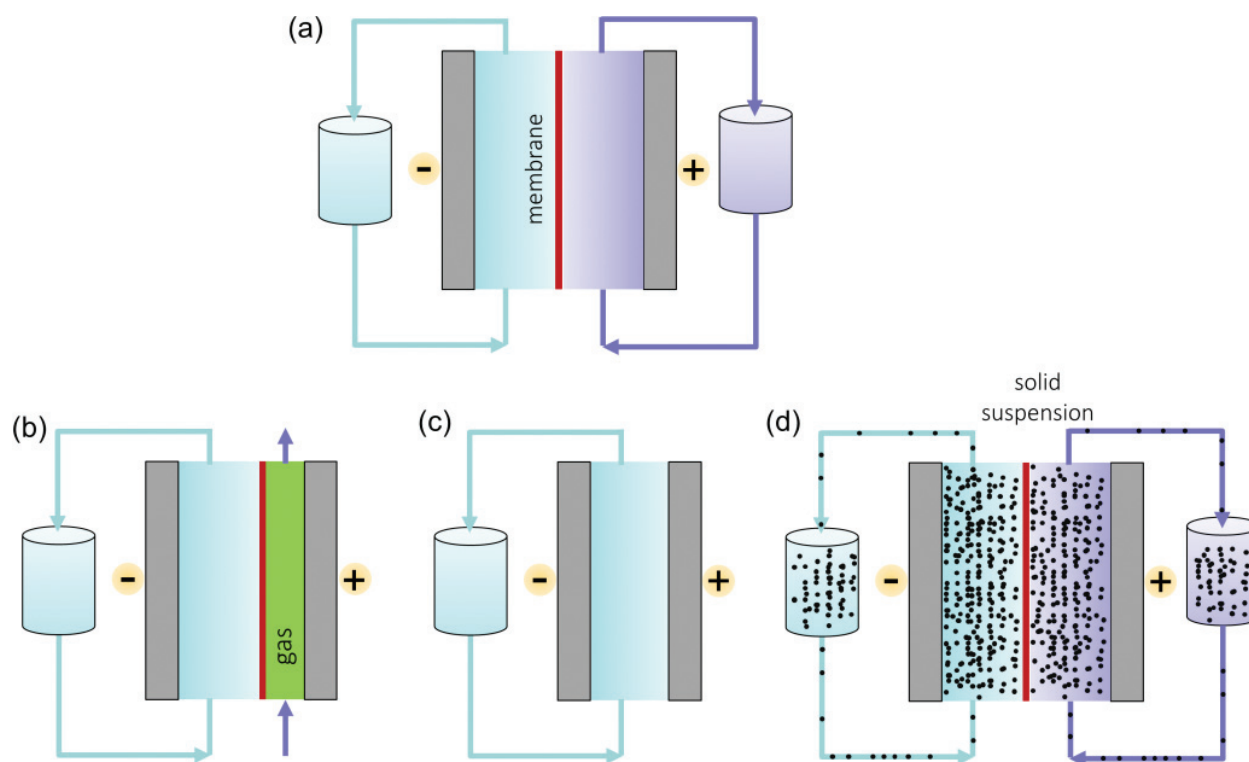


Figure 2. Configurations of (a) a conventional redox flow battery with two divided compartments containing dissolved active species, (b) a hybrid redox flow battery with gas supply at one electrode, (c) a redox flow battery with membrane-less structure and (d) a redox flow battery with solid particle suspension as flowing media.

Hybrid redox flow batteries such as zinc-bromine and zinc-cerium systems use metal stripping/plating reactions (Zn^{2+}/Zn , -0.76 V vs. [standard hydrogen electrode] SHE) on one of the electrodes inside the cell and the other side with normal soluble flowing electrolyte. Similarly, redox flow lithium batteries in non-aqueous electrolytes have been explored to make use of the low redox potential of Li^+/Li couple (-3.04 V vs. SHE). During charging, zinc or lithium is deposited from the electrolyte and during discharging, Zn^{2+} or Li^+ dissolves into the solution again. A shortcoming of such hybrid redox flow battery is that the energy storage capability is limited by the free space inside the cell accommodating the metal deposits.

A second-type hybrid redox flow batteries use gas such as Cl_2 , O_2 and H_2 as the reaction medium or with gas evolution reaction at the cathode or anode (**Figure 2b**). For instance, oxygen reduction reaction ($\text{O}_2 + 4\text{H}^+ + 4\text{e}^- \rightleftharpoons 2\text{H}_2\text{O}$) with high positive potential can be used as the cathode. The cell capacity is then only determined by the capacity of anolyte. Oxygen reduction reaction in non-aqueous electrolytes with the presence of lithium ions can proceed through: $\text{O}_2 + 2\text{Li}^+ + 2\text{e}^- \rightleftharpoons \text{Li}_2\text{O}_2$. Moreover, oxygen reduction and oxidation during discharging and charging can be catalysed chemically with redox mediators [5]. Interestingly, the use of electrocatalysts for the oxygen reduction and oxidation as in a conventional system can be avoided. Note that the formation and deposition of Li_2O_2 proceed at porous matrix, which can be held statically in a gas diffusion tank over charging/discharging. Such a concept may maintain the character of decoupled energy and power for flow batteries.

For aqueous electrolytes, oxygen and hydrogen gas evolution reactions by electrolysis of water take place during charging at very positive and negative electrode potentials, respectively.

Hydrogen evolution reaction has been observed as a parasitic side reaction at the anode for some flow battery systems. Such behaviour has been used to store electricity and to generate hydrogen simultaneously ($2V^{2+} + 2H^{+} \rightarrow H_2 + 2V^{3+}$) as demonstrated in a vanadium-cerium flow battery [6]. Hydrogen generated can be then used to produce electricity in fuel cells.

The ionic conductivity and selectivity of membranes often significantly affect the overall cell performance for many redox flow batteries. High area resistance of membrane restricts the practical operation only at low current densities. Crossover of active species through membrane leads to performance loss over cycling. Redox chemistry of active species with formation of electrodeposits leads to another type of cell configuration without membranes and with only one electrolyte reservoir [7] (**Figure 2c**). Some selected membrane-free redox flow batteries are listed in **Table 1** [8–14]. Reasonable energy efficiencies and cycling stability have been observed. Considering the high cost of most commercial ion exchange membranes, such membrane-free cell configuration could enable simple operation and cost-effective applications.

Deposited anodic species should have slow dissolution rate in the presence of oxidized catholyte species as a self-discharge reaction. A direct reaction between the deposited metal and the other electroactive species in the electrolyte should be negligible or inhibited. Self-discharge effects must be minimized compared to a targeted rapid charging/discharging reaction. Acidic-supporting electrolyte is not suitable for anodic metal deposition. Solid-phase reactions in general have poor kinetics, in comparison with those in liquid electrolytes. The voltage efficiencies in most of the membrane-free flow batteries are relatively low (60–80%) restricted by mass transport and charge transfer kinetics. Compared to the flow-by configuration, an undivided battery with flow-through electrodes may assure enhanced mass transport. However, the flow rate will be largely limited.

A laminar flow battery using two-liquid flowing media, pumped through a slim channel without lateral mixing or with very little mixing, enables membrane-free operation. H_2 (flowing across anode with pumped liquid hydrobromic acid) aqueous bromine laminar flow

| Flow batteries | Energy efficiencies | Cycling stability | Ref. |
|---------------------------------|---|---|------|
| Pb/PbO ₂ | 65% | Limited by the dendrite growth of Pb and formation of unwanted phase of β -PbO ₂ | [8] |
| Zn-NiOOH | 86% | Stable over 1000 cycles with ~600% Zn excess | [9] |
| Cu-PbO ₂ | About 83% at 20.8 mA cm ⁻² | Stable over 450 cycles | [10] |
| Zn-Ce | About 75% at 20 mA cm ⁻² | Limited by Zn negative electrode, Zn residual on electrode after discharge | [11] |
| Zn-Quinone | About 40–70% at 30 mA cm ⁻² | Stable for low concentration quinone (50 mM) | [12] |
| H ₂ -Br ₂ | High round-trip efficiency at high current density up to 1 A cm ⁻² | Not given | [13] |
| Symmetric Ru(acac) ₃ | About 20% at about 2 mA cm ⁻² | Low coulombic and voltage efficiencies | [14] |

Table 1. Membrane-free redox flow batteries.

battery demonstrated herewith allows high concentration reactants, fast reaction rates and a high peak power density (0.795 W cm^{-2}) [13].

Among various electrical energy storage technologies, redox flow batteries generally have relatively low energy density (for instance about 30 Wh L^{-1} for all-vanadium redox flow batteries). Thus, although recharging the electrolyte can be done by replacing the depleted one within a few minutes of transportation applications, redox flow batteries are only considered to be used in stationary energy storage. To increase the energy density, highly water-soluble species for instance LiI (solubility up to 8.2 M) and ZnI (7 M) can potentially enhance the volumetric energy density. The use of concentrated ZnI electrolyte leads to a high theoretical energy density of 322 Wh L^{-1} [15], which may even rival batteries based on lithium-ion chemistry (LiFePO₄ cathode, 223 Wh L^{-1}).

Another successful development is the redox flow lithium batteries. Pulverized energy-dense solid electrode materials such as LiCoO₂ and LiFePO₄ can be suspended in a flowable slurry, which is then circulated like a liquid-soluble electrolyte (**Figure 2d**). Due to the high molar concentration of lithium in the solid materials (for instance about 51.2 M for LiCoO₂ and 22.8 M for LiFePO₄, compared to about 1.6 M for vanadium species in conventional vanadium redox flow batteries), such flow batteries allow high volumetric energy density (about 580 Wh L^{-1} have been achieved [16]). Thus, redox flow batteries may find applications even in portable electronics and electric vehicles.

4. Redox electrochemistry of flow batteries

The overall system performance and cost for redox flow batteries depend largely on the flow cell redox electrochemistry. Great efforts have been made in search of alternative battery chemistry from electrolytes to electrodes [4, 17, 18]. The possible cell voltage depends on the selected redox couples (**Table 2**) and is limited by the electrochemical window of a given solvent-electrode system, stability of the supporting cation or anion and stability of the bipolar plate materials (**Figure 3**).

Table 2 summarises the electrochemical redox reactions at cathode and anode and cell open circuit voltage (OCV) for various reported redox flow batteries. For aqueous electrolytes, the typical cell voltage is below 1.5 V. To achieve high cell voltage, organic solvents with a broad electrochemical window such as acetonitrile (6.1 V) and propylene carbonate (6.6 V) are needed [4]. However, most of the used active species have poor solubility in organic solvents. High cell voltage in this case comes at the expense of low concentration of active species. A compromise among the solubility, cell voltage, reaction kinetics and suitable working temperature should be reached for selecting a suitable electrolyte. Ce⁴⁺/Ce³⁺ redox reaction (from 1.44 to 1.70 V vs. SHE, depending on the type of supporting acidic electrolyte), occurring at potential beyond the stability limit of bipolar plate (**Figure 3**), needs special electrodes such as catalyst-coated titanium plate or mesh.

Many anodic reactions have low negative potential; the applications in aqueous batteries can be hindered by H₂ evolution due to the electrolysis of water with unwanted energy loss and an

| Cathode redox reactions | Anode redox reactions | Cell OCV/V |
|--|--|-----------------------------------|
| $\text{Br}_2 + 2\text{e}^- \rightleftharpoons 2\text{Br}^-$ or $\text{Br}_3^- + 2\text{e}^- \rightleftharpoons 3\text{Br}^-$ | $\text{AQDSH} \rightleftharpoons \text{AQDS}^- + \text{H}^+ + \text{e}^-$ | 0.86 |
| $[\text{Mn}(\text{acac})_3]^+ + \text{e}^- \rightleftharpoons \text{Mn}(\text{acac})_3$ | $[\text{Mn}(\text{acac})_3]^- \rightleftharpoons \text{Mn}(\text{acac})_3 + \text{e}^-$ | 1.10 |
| $\text{Fe}^{3+} + \text{e}^- \rightleftharpoons \text{Fe}^{2+}$ | $\text{Cr}^{2+} \rightleftharpoons \text{Cr}^{3+} + \text{e}^-$ | 1.19 |
| $\text{VO}_2^+ + 2\text{H}^+ + \text{e}^- \rightleftharpoons \text{VO}^{2+} + \text{H}_2\text{O}$ | $\text{V}^{2+} \rightleftharpoons \text{V}^{3+} + \text{e}^-$ | 1.26 |
| $\text{I}_3^- + 2\text{e}^- \rightleftharpoons 3\text{I}^-$ | $\text{Zn} \rightleftharpoons \text{Zn}^{2+} + 2\text{e}^-$ | 1.30 |
| $\text{PbO}_2 + 4\text{H}^+ + \text{SO}_4^{2-} + 2\text{e}^- \rightleftharpoons \text{PbSO}_4 + 2\text{H}_2\text{O}$ | $\text{Cu} \rightleftharpoons \text{Cu}^{2+} + 2\text{e}^-$ | 1.35 |
| $\text{ClBr}_2^{2-} + \text{e}^- \rightleftharpoons 2\text{Br}^- + \text{Cl}^-$ | $\text{VBr}_2 + \text{Br}^- \rightleftharpoons \text{VBr}_3 + \text{e}^-$ | 1.35 |
| $\text{Br}_2 + 2\text{e}^- \rightleftharpoons 2\text{Br}^-$ or $\text{Br}_3^- + 2\text{e}^- \rightleftharpoons 3\text{Br}^-$ | $2\text{S}_2^{2-} \rightleftharpoons \text{S}_4^{2-} + 2\text{e}^-$ | 1.36 |
| hydroquinone \rightleftharpoons | $\text{Zn} \rightleftharpoons \text{Zn}^{2+} + 2\text{e}^-$ | 1.40 |
| <i>para</i> -benzoquinone + $2\text{H}^+ + 2\text{e}^-$ | | |
| $\text{O}_2 + 4\text{H}^+ + 4\text{e}^- \rightleftharpoons 2\text{H}_2\text{O}$ | $\text{V}^{2+} \rightleftharpoons \text{V}^{3+} + \text{e}^-$ | 1.49 |
| $[\text{Fe}(\text{CN})_6]^{3-} + \text{e}^- \rightleftharpoons [\text{Fe}(\text{CN})_6]^{4-}$ | $\text{Zn} + 4\text{OH}^- \rightleftharpoons [\text{Zn}(\text{OH})_4]^{2-} + 2\text{e}^-$ | 1.58 |
| $\text{PbO}_2 + 4\text{H}^+ + 2\text{e}^- \rightleftharpoons \text{Pb}^{2+} + 2\text{H}_2\text{O}$ | $\text{Pb} \rightleftharpoons \text{Pb}^{2+} + 2\text{e}^-$ | 1.69 |
| $2\text{NiOOH} + 2\text{H}_2\text{O} + 2\text{e}^- \rightleftharpoons 2\text{Ni}(\text{OH})_2$ | $\text{Zn} + 4\text{OH}^- \rightleftharpoons [\text{Zn}(\text{OH})_4]^{2-} + 2\text{e}^-$ | 1.70 |
| $\text{TEMPO}^+ + \text{e}^- \rightleftharpoons \text{TEMPO}^\bullet$ | $\text{Zn} \rightleftharpoons \text{Zn}^{2+} + 2\text{e}^-$ | 1.70 |
| $\text{VO}_2^+ + 2\text{H}^+ + \text{e}^- \rightleftharpoons \text{VO}^{2+} + \text{H}_2\text{O}$ | $\text{Zn} \rightleftharpoons \text{Zn}^{2+} + 2\text{e}^-$ | 1.76 |
| $[\text{Ru}(\text{acac})_3]^+ + \text{e}^- \rightleftharpoons \text{Ru}(\text{acac})_3$ | $[\text{Ru}(\text{acac})_3]^- \rightleftharpoons \text{Ru}(\text{acac})_3 + \text{e}^-$ | 1.77 |
| $\text{Br}_2 + 2\text{e}^- \rightleftharpoons 2\text{Br}^-$ or $\text{Br}_3^- + 2\text{e}^- \rightleftharpoons 3\text{Br}^-$ | $\text{Zn} \rightleftharpoons \text{Zn}^{2+} + 2\text{e}^-$ | 1.82 |
| $\text{Cl}_2 + 2\text{e}^- \rightleftharpoons 2\text{Cl}^-$ | $\text{Zn} \rightleftharpoons \text{Zn}^{2+} + 2\text{e}^-$ | 2.12 |
| $\text{ClBr}_2^- + 2\text{e}^- \rightleftharpoons 2\text{Br}^- + \text{Cl}^-$ | $\text{Zn} \rightleftharpoons \text{Zn}^{2+} + 2\text{e}^-$ | 2.16 |
| $[\text{V}(\text{acac})_3]^+ + \text{e}^- \rightleftharpoons \text{V}(\text{acac})_3$ | $[\text{V}(\text{acac})_3]^- \rightleftharpoons \text{V}(\text{acac})_3 + \text{e}^-$ | 2.18 |
| $\text{Ce}^{4+} + \text{e}^- \rightleftharpoons \text{Ce}^{3+}$ | $\text{Zn} \rightleftharpoons \text{Zn}^{2+} + 2\text{e}^-$ | 2.20–2.46 |
| $[\text{Fe}(\text{bpy})_3]^{3+} + \text{e}^- \rightleftharpoons [\text{Fe}(\text{bpy})_3]^{2+}$ | $[\text{Ni}(\text{bpy})_3] \rightleftharpoons [\text{Ni}(\text{bpy})_3]^{2+} + \text{e}^-$ | 2.30 |
| $\text{Rubrene}^{\bullet+} + \text{e}^- \rightleftharpoons \text{Rubrene}$ | $\text{Rubrene}^{\bullet-} \rightleftharpoons \text{Rubrene} + \text{e}^-$ | 2.30 |
| $[\text{Ru}(\text{bpy})_3]^{3+} + \text{e}^- \rightleftharpoons [\text{Ru}(\text{bpy})_3]^{2+}$ | $[\text{Ru}(\text{bpy})_3]^+ \rightleftharpoons [\text{Ru}(\text{bpy})_3]^{2+} + \text{e}^-$ | 2.60 |
| $[\text{Cr}(\text{acac})_3]^+ + \text{e}^- \rightleftharpoons \text{Cr}(\text{acac})_3$ | $[\text{Cr}(\text{acac})_3]^- \rightleftharpoons \text{Cr}(\text{acac})_3 + \text{e}^-$ | 3.40 |
| $[\text{Fe}(\text{CN})_6]^{3-} + \text{e}^- \rightleftharpoons [\text{Fe}(\text{CN})_6]^{4-}$ | $\text{Li} \rightleftharpoons \text{Li}^+ + \text{e}^-$ | 3.40 |
| $\text{OFN}^{\bullet+} + \text{e}^- \rightleftharpoons \text{OFN}$ | $\text{BP}^{\bullet-} \rightleftharpoons \text{BP} + \text{e}^-$ | 4.52 |
| $4\text{Ce}^{4+} + 2\text{H}_2\text{O} \rightarrow 4\text{Ce}^{3+} + 4\text{H}^+ + \text{O}_2$ | $2\text{V}^{2+} + 2\text{H}^+ \rightarrow \text{H}_2 + 2\text{V}^{3+}$ | Cell is chemically discharged [6] |

Table 2. Selected redox reactions and cell OCV for redox flow batteries.

imbalance in the state of charge between two sides of the batteries. Through using concentrated electrolytes of water-in-ionic liquid (water in 1-butyl-3-methylimidazolium chloride, BMImCl) [19, 20] or water-in-salt (water in lithium, bis(trifluoromethylsulphonyl)imide, LiTFSI) [21], the onset of oxygen evolution and hydrogen reactions can be shifted to more positive and negative potentials, respectively. Broad electrochemical window of about 3 V has been achieved accordingly (Figure 3). It is considered that the amount of free water molecules reduces at such

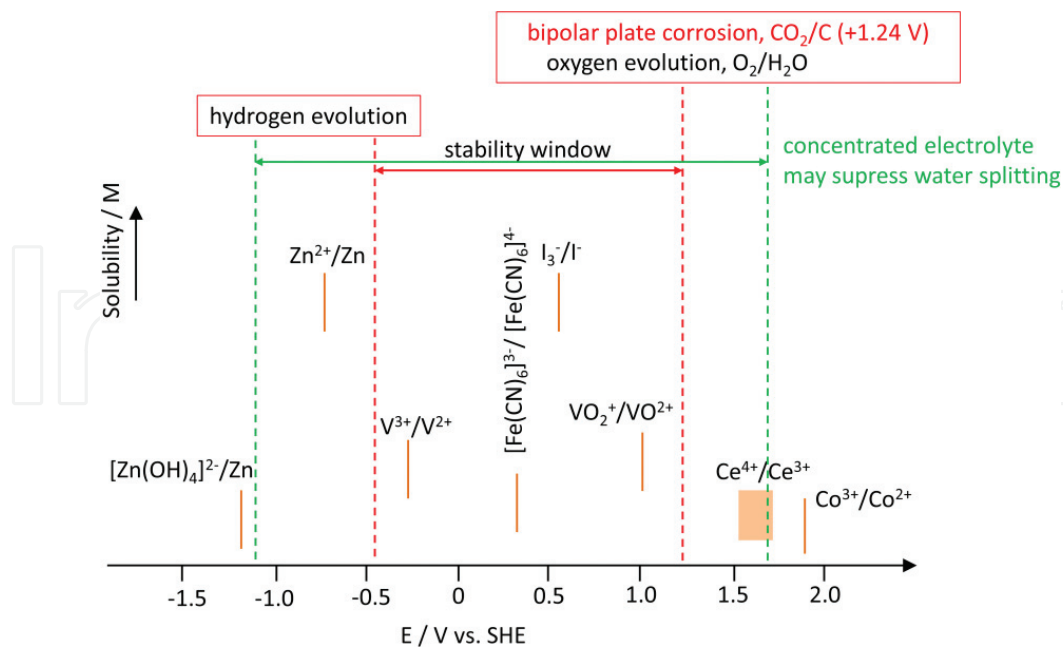


Figure 3. Potentials and relative solubility of selected inorganic and organic redox couples for redox flow batteries. Dotted lines show the electrochemical stability limit of typical aqueous electrolytes. Dashed lines show the possibility to extend the stability limit for aqueous electrolytes using concentrated electrolytes [19, 21].

concentrated mixtures. The inner Helmholtz layer close to the electrode surface is mostly occupied by the $[\text{BMIm}]^+$ cation or TFSI^- anion, respectively. Water decomposition is then largely inhibited. The redox potentials for hydrogen and oxygen evolution reactions are pH dependent. Individual control in the pH values of the anolyte and catholyte with a multi-membrane system leads to high cell operation voltage of about 3 V [22].

In contrast to the electrochemical stability of the redox species and solvents, chemical stability of electroactive species and cell components is also critical for long-term operation. Vanadium electrolytes form solid precipitates at a temperature above 40 or below 10°C at concentrations above 1.6 M for all-vanadium redox flow batteries. Oxidizing V^{5+} and Ce^{4+} may cause degradation of membrane and the graphite electrode materials. Complexing agents are needed to store bromine, whereas phase separation (formation of water-insoluble emulsion) occurs for bromine complexes during charging for bromine-based flow batteries. Cross-contamination in bromine-polysulphide batteries may generate heat and release toxic Br_2 and H_2S .

High rate performance of redox flow batteries means high power generation capability. Ideally, two active species at both sides of the cell are expected to have close rate constants. However, mismatches in reaction rates are often observed. For many electrode reactions with sluggish kinetics, catalysts are needed to reduce the polarization (i.e. to improve the voltage efficiencies) and to improve the reaction rate (**Table 3**) [23]. Catalysts are generally applied onto a porous material, which offers high contact area for electrolytes. The supporting materials should have high electrical conductivity, mechanical stability, reasonable cost and high levels of oxygen and hydrogen evolution overpotential for aqueous system. Carbon-based materials are commonly used for this purpose [24].

| Electrode reactions | Catalysts |
|---|--|
| $\text{VO}_2^+ + 2\text{H}^+ + \text{e}^- \rightleftharpoons \text{VO}^{2+} + \text{H}_2\text{O}$ | $\text{Mn}_3\text{O}_4/\text{carbon fibre}$ ZrO_2 Bi_2O_3 Nanorod Nb_2O_5 Ir-modification of carbon felt WO_3 PbO_2 |
| $\text{V}^{3+} + \text{e}^- \rightleftharpoons \text{V}^{2+}$ | $\text{Mn}_3\text{O}_4/\text{carbon fibre}$ ZrO_2 Bi_2O_3 Nanorod Nb_2O_5 TiC |
| $\text{Cr}^{3+} + \text{e}^- \rightleftharpoons \text{Cr}^{2+}$ | Noble catalysts |
| $\text{Ce}^{4+} + \text{e}^- \rightarrow \text{Ce}^{3+}$ | Platinized titanium |
| $\text{Cl}_2 + 2\text{e}^- \rightleftharpoons 2\text{Cl}^-$ | RuO_2 |
| $\text{O}_2 + 4\text{H}^+ + 4\text{e}^- \rightleftharpoons 2\text{H}_2\text{O}$ | Pt/Ir mixed oxide |

Table 3. Catalysts used for redox couple reactions.

5. Redox active organic electrolytes

Compared to the metal-based electrolytes for redox flow batteries with limited number and resource, organic molecules with unlimited chemical space allow low-cost (for instance, from \$5–10 kg^{−1} vs. \$27 kg^{−1} for vanadium) and high-performance operation. Fast reaction kinetics of organic compounds permit high power generation. High solubility can be realized by controlling the solubilizing functional groups. Redox potentials can be adjusted by varying the electron-donating (−OH, −NH₂) or -accepting (−SO₃H, −NO₂, −PO₃H₂) properties of the functional groups. By tuning the molecule size or grafting polymer chains, low membrane crossover can be obtained. High-performance organic-based aqueous redox flow batteries have been demonstrated recently (Table 4) [25–30].

Quinone-based organic compounds have received great attention, ranging from simple hydroquinone to large anthraquinone. These materials have merits of low cost and fast reaction rates. A peak power density of 1 W cm^{−2} has been observed for a 9,10-anthraquinone-2,7-disulfonic acid (AQDS)-bromide system [31], which is close to a reported peak power density of 1.34 W cm^{−2} for vanadium redox flow batteries. Compared to the relative small molecules such as hydroquinone and 2,2,6,6-tetramethylpiperidine 1-oxyl (TEMPO), large molecules such as AQDS and methyl viologen (MV) are expected to have low-membrane crossover rates. Functionalization of these active organic compounds with polymer backbone chains further enables the battery operation with low-cost size-exclusion membranes [32]. The development

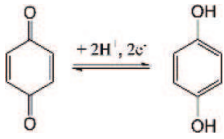
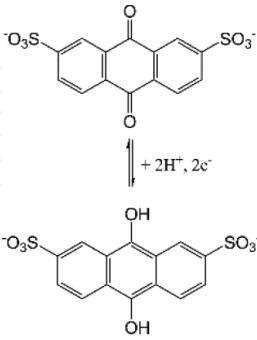
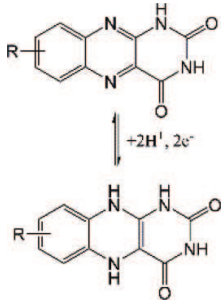
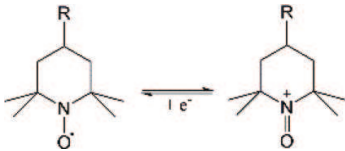
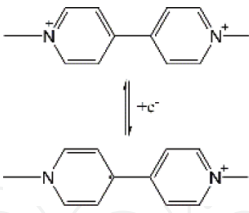
| Reaction mechanisms | Redox reactions | Redox potential/V vs. SHE | Ref. |
|---------------------------------|---|---|------|
| $2e^-$, $2H^+$ redox reactions |  | pH dependent, ranging from 0.56 to 0.75 | [25] |
| $2e^-$, $2H^+$ redox reactions |  | 0.2 | [26] |
| $2e^-$, $2H^+$ redox reactions |  | -0.73 for R = OH | [27] |
| Organic radicals |  | About 0.5 V in carbonate electrolyte | [28] |
| Organic radicals |  | -0.45 V | [29] |
| Organodisulfide | $R-S-S-R \rightleftharpoons 2 R-S^{\cdot}$ | About -1 V | [30] |

Table 4. Selected redox active organic compounds used for redox flow batteries.

of organic active materials for redox flow batteries holds great promise for stationary electrochemical energy storage.

6. Semi-solid redox flow batteries

To overcome the restrictions in solubility of active species in liquid electrolytes, suspensions with energy-dense solid materials have been introduced for redox flow batteries. The concept

was first demonstrated with intercalation materials by Chiang et al. [33], which are typically used for lithium ion batteries. Such semi-solid lithium redox flow batteries combine the merits of high energy density for lithium ion batteries and the decoupled character of conventional redox flow batteries. In order to form a percolation network for charge transfer, several strategies have been proposed: (i) dispersing conductive additive such as carbon into the electrolytes, (ii) adding redox mediators and (iii) inserting a metal wire as a current collector [34]. It has been found that the conductive electrolytes encounter the issue of shunt current between cells in a stack.

Energy-dense batteries, based on lithiation chemistry and intercalation chemistry of abundant elements (such as Na, Mg and Al etc.), contribute significantly to the transportable applications of various electronic devices and revolution of our modern societies. The successful development in these materials raises opportunities in new applications for flow batteries. Li-, Na- and organic molecule-based semi-solid redox flow batteries have been developed recently (Table 5) [33–37]. For a pumping system with solid suspension, the rheological properties of suspension need to be considered.

In contrast to the flow batteries with both (de)lithiation and electron transfer reactions occurring inside the electrochemical cells (Figure 2d), a new concept using redox shuttle molecules has been introduced [38], wherein solid active materials are kept statically in the tank and only the shuttle molecules are circulated in the electrochemical cell (Figure 4). Electrochemical redox reactions of the shuttle molecules go on at the electrode inside the cell, whereas chemical (de)lithiation of the active solid materials in the tank occurs through the reactions between the solid materials and the shuttle molecules. Since the active solid materials are not involved in the electrochemical reaction, conductive additives (such as carbon black) are not necessary in such a system. In addition, low concentration shuttle molecules of only several mM are sufficient to induce the (de)lithiation reaction of a large amount of solid materials.

| Semi-solid flow batteries | Suspension | Remarks | Ref. |
|---|--|---|------|
| LiCoO ₂ /Li ₄ Ti ₅ O ₁₂ | 26 vol% LiCoO ₂ , 0.8 vol% Ketjen; 25 vol% Li ₄ Ti ₅ O ₁₂ , 0.8 vol% Ketjen | C/3 to C/8 rate, high energy efficiency | [33] |
| LiCoO ₂ /Li ₄ Ti ₅ O ₁₂ | Carbon-free 0.5 vol% LiCoO ₂ , 1 vol% Li ₄ Ti ₅ O ₁₂ | Low current density from 0.002 to 0.008 mA cm ⁻² , low coulombic efficiency of about 11.5% | [34] |
| P2-type Na _x Ni _{0.22} Co _{0.11} Mn _{0.66} O ₂ / NaTi ₂ (PO ₄) ₃ | Active material with 1.3 wt% conductive additive | Current density below 0.5 mA cm ⁻² , low voltage efficiency of about 40%, energy density of about 9 Wh L ⁻¹ | [35] |
| Symmetric battery with polythiophene | Polythiophene (8.41 g L ⁻¹), Ketjenblack (2 g L ⁻¹) | Low current density (<1 mA cm ⁻²), energy efficiency of 60.9% at 0.5 mA cm ⁻² | [36] |
| Zn/polyaniline | 10 wt% polyaniline powder in suspension | 0.28 V overpotential at 20 mA cm ⁻² | [37] |

Table 5. Selected examples for semi-solid redox flow batteries.

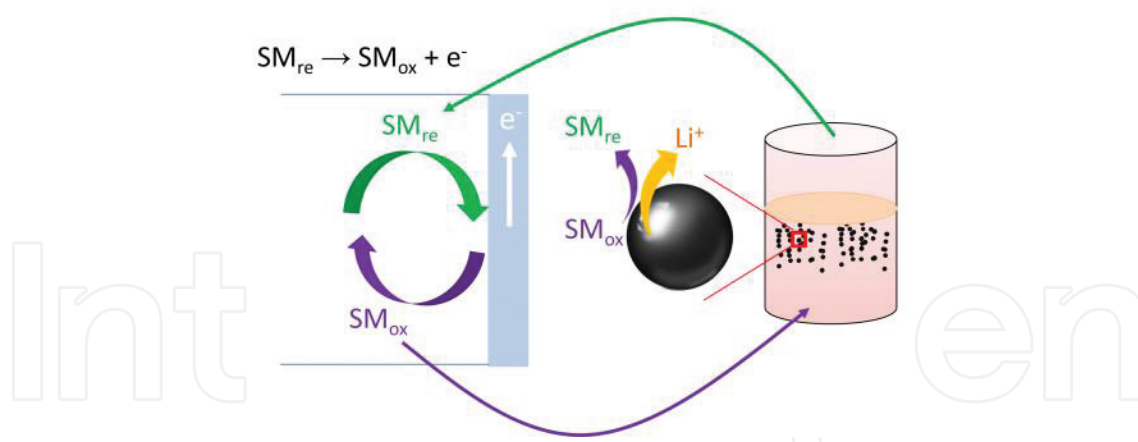


Figure 4. An illustration of a semi-solid redox flow battery with solid materials stored statically in the tank, and redox shuttle molecule (SM) circulated with electrolyte.

7. Conclusions and perspectives

Redox flow battery technology is relatively new and not yet well-developed. Rational electrolyte management and cell design can lead to the enhancement of energy storage capability and a reduction in construction cost. Novel electrolyte chemistry and development of a new configuration of flow batteries will create high system flexibility. Physiochemical and electrochemical redox properties of active couples, stability window of supporting electrolyte, selection of supporting ions, stability of electrode materials and cell components are key factors for successful applications. Future market penetration of flow batteries needs low cost, high energy density and high power density. The pace of recent development in the active organic molecules as electrolytes opens new strategies of cost-effective and sustainable solutions for large-scale stationary energy storage. The application of energy-dense solid materials in suspension for redox flow batteries may largely enhance the energy density of flow battery systems.

Acknowledgements

We thank the support from the basic research funding of KIST Europe (“Electrochemical energy transformation and energy storage”). Ruiyong Chen thanks Professor R. Hempelmann for his continuing support.

Abbreviations

| | |
|------------------|--|
| AQDS | 9,10-Anthraquinone-2,7-disulphonic acid |
| BMIImCl | 1-Butyl-3-methylimidazolium chloride |
| BP | Biphenyl |
| BP ^{•-} | Biphenyl radical anion |
| LiTFSI | Lithium bis(trifluoromethylsulphonyl)imide |

| | |
|-------------------|--------------------------------------|
| MV | Methyl viologen dichloride |
| OCV | Open circuit voltage |
| OFN | Octafluoronaphthalene |
| OFN ^{•+} | Octafluoronaphthalene radical cation |
| SHE | Standard hydrogen electrode |
| TEMPO | 2,2,6,6-Tetramethylpiperidine 1-oxyl |

Author details

Ruiyong Chen^{1,2*}, Sangwon Kim^{1,2} and Zhenjun Chang^{1,2,3}

*Address all correspondence to: r.chen@kist-europe.de

1 Transfercenter Sustainable Electrochemistry, Saarland University, Saarbrücken, Germany

2 Korea Institute of Science and Technology (KIST) Europe, Saarbrücken, Germany

3 College of Materials Science and Engineering, Jiangsu University of Science and Technology, Zhenjiang, China

References

- [1] Skyllas-Kazacos M, Rychcik M, Robins RG, Fane AG, Green MA. New all-vanadium redox flow cell. *Journal of the Electrochemical Society*. 1986;**133**:1057–1058. DOI: 10.1149/1.2108706
- [2] Tang A, Bao J, Skyllas-Kazacos M. Thermal modelling of battery configuration and self-discharge reactions in vanadium redox flow battery. *Journal of Power Sources*. 2012;**216**: 489–501. DOI: 10.1016/j.jpowsour.2012.06.052
- [3] Liu H, Xu Q, Yan C, Qiao Y. Corrosion behavior of a positive graphite electrode in vanadium redox flow battery. *Electrochimica Acta*. 2011;**56**:8783–8790. DOI: 10.1016/j.electacta.2011.07.083
- [4] Gong K, Fang Q, Gu S, Li SFY, Yan Y. Nonaqueous redox-flow batteries: Organic solvents, supporting electrolytes, and redox pairs. *Energy & Environmental Science*. 2015;**8**: 3515–3530. DOI: 10.1039/c5ee02341f
- [5] Zhu YG, Jia C, Yang J, Pan F, Huang Q, Wang Q. Dual redox catalysts for oxygen reduction and evolution reactions: Towards a redox flow Li–O₂ battery. *Chemical Communications*. 2015;**51**:9451–9454. DOI: 10.1039/c5cc01616a
- [6] Amstutz V, Toghiani KE, Powlesland F, Vrubel H, Comninellis C, Hu X, Girault HH. Renewable hydrogen generation from a dual-circuit redox flow battery. *Energy & Environmental Science*. 2014;**7**:2350–2358. DOI: 10.1039/c4ee00098f

- [7] Bamgbopa MO, Almheiri S, Sun H. Prospects of recently developed membraneless cell designs for redox flow batteries. *Renewable and Sustainable Energy Reviews*. 2017;**70**: 506–518. DOI: 10.1016/j.rser.2016.11.234
- [8] Hazza A, Pletcher D, Wills R. A novel flow battery: A lead acid battery based on an electrolyte with soluble lead (II). Part I. Preliminary studies. *Physical Chemistry Chemical Physics*. 2004;**6**:1773–1778. DOI: 10.1039/b401115e
- [9] Cheng J, Zhang L, Yang Y-S, Wen Y-H, Cao G-P, Wang X-D. Preliminary study of single flow zinc-nickel battery. *Electrochemistry Communications*. 2007;**9**:2639–2642. DOI: 10.1016/j.elecom.2007.08.016
- [10] Pan J, Sun Y, Cheng J, Wen Y, Yang Y, Wan P. Study on a new single flow acid Cu–PbO₂ battery. *Electrochemistry Communications*. 2008;**10**:1226–1229. DOI: 10.1016/j.elecom.2008.06.008
- [11] Leung PK, de León CP, Walsh FC. An undivided zinc-cerium redox flow battery operating at room temperature (295 K). *Electrochemistry Communications*. 2011;**13**:770–773. DOI: 10.1016/j.elecom.2011.04.011
- [12] Leung PK, Martin T, Shah AA, Anderson MA, Palma J. Membrane-less organic–inorganic aqueous flow batteries with improved cell potential. *Chemical Communications*. 2016;**52**: 14270–14273. DOI: 10.1039/c6cc07692k
- [13] Braff WA, Bazant MZ, Buie CR. Membrane-less hydrogen bromine flow battery. *Nature Communications*. 2013;**4**:2346. DOI: 10.1038/ncomms3346
- [14] Chakrabarti MH, Roberts EPL, Bae C, Saleem M. Ruthenium based redox flow battery for solar energy storage. *Energy Conversion and Management*. 2011;**52**:2501–2508. DOI: 10.1016/j.enconman.2011.01.012
- [15] Li B, Nie Z, Vijayakumar M, Li G, Liu J, Sprenkle V, Wang W. Ambipolar zinc-polyiodide electrolyte for a high-energy density aqueous redox flow battery. *Nature Communications*. 2015;**6**:6303. DOI: 10.1038/ncomms7303
- [16] Chen H, Lu Y-C. A high-energy-density multiple redox semi-solid–liquid flow battery. *Advanced Energy Materials*. 2016;**6**:1502183. DOI: 10.1002/aenm.201502183
- [17] Pan F, Wang Q. Redox species of redox flow batteries: A review. *Molecules*. 2015;**20**:20499–20517. DOI: 10.3390/molecules201119711
- [18] Noack J, Roznyatovskaya N, Herr T, Fischer P. The chemistry of redox-flow batteries. *Angewandte Chemie International Edition*. 2015;**54**:9776–9809. DOI: 10.1002/anie.201410823
- [19] Chen R, Hempelmann R. Ionic liquid-mediated aqueous redox flow batteries for high voltage applications. *Electrochemistry Communications*. 2016;**70**:56–59. DOI: 10.1016/j.elecom.2016.07.003

- [20] Chen R, Hempelmann R. Ionic liquids-mediated aqueous electrolytes for redox flow batteries. In: 7th International Flow Battery Forum (IFBF). Swanbarton Limited, United Kingdom, 2016; 22-23. ISBN: 978-0-9571055-6-0
- [21] Suo L, Borodin O, Gao T, Olguin M, Ho J, Fan X, Luo C, Wang C, Xu K. "Water-in-salt" electrolyte enables high-voltage aqueous lithium-ion chemistries. *Science*. 2015;**350**:938–943. DOI: 10.1126/science.aab1595
- [22] Gu S, Gong K, Yan EZ, Yan Y. A multiple ion-exchange membrane design for redox flow batteries. *Energy & Environmental Science*. 2014;**7**:2986–2998. DOI: 10.1039/c4ee00165f
- [23] Park M, Ryu J, Cho J. Nanostructured electrocatalysts for all-vanadium redox flow batteries. *Chemistry – An Asian Journal*. 2015;**10**:2096–2110. DOI: 10.1002/asia.201500238
- [24] Chakrabarti MH, Brandon NP, Hajimolana SA, Tariq F, Yufit V, Hashim MA, Hussain MA, Low CTJ, Aravind PV. Application of carbon materials in redox flow batteries. *Journal of Power Sources*. 2014;**253**:150–166. DOI: 10.1016/j.jpowsour.2013.12.038
- [25] Ding Y, Yu G. A bio-inspired, heavy-metal-free, dual-electrolyte liquid battery towards sustainable energy storage. *Angewandte Chemie International Edition*. 2016;**55**:4772–4776. DOI: 10.1002/anie.201600705
- [26] Huskinson B, Marshak MP, Suh C, Er S, Gerhardt MR, Galvin CJ, Chen X, Aspuru-Guzik A, Gordon RG, Aziz MJ. A metal-free organic–inorganic aqueous flow battery. *Nature*. 2014;**505**:195–198. DOI: 10.1038/nature12909
- [27] Lin K, Gómez-Bombarelli R, Beh ES, Tong L, Chen Q, Valle A, Aspuru-Guzik A, Aziz MJ, Gordon RG. A redox-flow battery with an alloxazine-based organic electrolyte. *Nature Energy*. 2016;**1**:16102. DOI: 10.1038/nenergy.2016.102
- [28] Wei X, Xu W, Vijayakumar M, Cosimbescu L, Liu T, Sprenkle V, Wang W. TEMPO-based catholyte for high-energy density nonaqueous redox flow batteries. *Advanced Materials*. 2014;**26**:7649–7653. DOI: 10.1002/adma.201403746
- [29] Liu T, Wei X, Nie Z, Sprenkle V, Wang W. A total organic aqueous redox flow battery employing a low cost and sustainable methyl viologen anolyte and 4-HO-TEMPO catholyte. *Advanced Energy Materials*. 2016;**6**:1501449. DOI: 10.1002/aenm.201501449
- [30] Li B, Liu J. Progress and directions in low-cost redox flow batteries for large-scale energy storage. *National Science Review*. 2017; 4: 91–105. DOI: 10.1093/nsr/nww098
- [31] Chen Q, Eisenach L, Aziz MJ. Cycling analysis of a quinone-bromide redox flow battery. *Journal of the Electrochemical Society*. 2016;**163**:A5057–A5063. DOI: 10.1149/2.0081601jes
- [32] Winsberg J, Janoschka T, Morgenstern S, Hagemann T, Muench S, Hauffman G, Gohy J-F, Hager MD, Schubert US. Poly(TEMPO)/zinc hybrid-flow battery: A novel, "green," high voltage, and safe energy storage system. *Advanced Materials*. 2016;**28**:2238–2243. DOI: 10.1002/adma.201505000

- [33] Duduta M, Ho B, Wood VC, Limthongkul P, Brunini VE, Carter WC, Chiang Y-M. Semi-solid lithium rechargeable flow battery. *Advanced Energy Materials*. 2011;**1**:511–516. DOI: 10.1002/aenm.201100152
- [34] Qi Z, Liu AL, Koenig Jr GM. Carbon-free solid dispersion LiCoO_2 redox couple characterization and electrochemical evaluation for all solid dispersion redox flow batteries. *Electrochimica Acta*. 2017;**228**:91–99. DOI: 10.1016/j.electacta.2017.01.061
- [35] Ventosa E, Buchholz D, Klink S, Flox C, Chagas LG, Vaalma C, Schuhmann W, Passerini S, Morante JR. Non-aqueous semi-solid flow battery based on Na-ion chemistry. P2-type $\text{Na}_x\text{Ni}_{0.22}\text{Co}_{0.11}\text{Mn}_{0.66}\text{O}_2\text{-NaTi}_2(\text{PO}_4)_3$. *Chemical Communications*. 2015;**51**:7298–7301. DOI: 10.1039/c4cc09597a
- [36] Oh SH, Lee C-W, Chun DH, Jeon J-D, Shim J, Shin KH, Yang JH. A metal-free and all-organic redox flow battery with polythiophene as the electroactive species. *Journal of Materials Chemistry A*. 2014;**2**:19994–19998. DOI: 10.1039/c4ta04730c
- [37] Wu S, Zhao Y, Li D, Xia Y, Si S. An asymmetric Zn//Ag doped polyaniline microparticle suspension flow battery with high discharge capacity. *Journal of Power Sources*. 2015; **275**:305–311. DOI: 10.1016/j.jpowsour.2014.11.012
- [38] Huang Q, Li H, Grätzel M, Wang Q. Reversible chemical delithiation/lithiation of LiFePO_4 : Towards a redox flow lithium-ion battery. *Physical Chemistry Chemical Physics*. 2013;**15**:1793–1797. DOI: 10.1039/c2cp44466f